



Time-Dependent Predominance of Nonhomologous DNA End-Joining Pathways during Embryonic Development in Mice

Kishore K. Chiruvella¹†, Robin Sebastian¹†, Sheetal Sharma¹,
Anjali A. Karande¹, Bibha Choudhary^{1,2*} and Sathees C. Raghavan^{1*}

¹Department of Biochemistry, Indian Institute of Science, Bangalore 560 012, India

²Institute of Bioinformatics and Applied Biotechnology, Biotech Park, Electronics City, Bangalore 560 100, India

Received 21 December 2011;
received in revised form
18 January 2012;
accepted 20 January 2012
Available online
27 January 2012

Edited by M. Yaniv

Keywords:

NHEJ;
double-strand break repair;
DNA damage;
genomic instability;
cell-free repair system

Repair of DNA double-strand breaks (DSBs) is crucial for maintaining genomic integrity during the successful development of a fertilized egg into a whole organism. To date, the mechanism of DSB repair in postimplantation embryos has been largely unknown. In the present study, using a cell-free repair system derived from the different embryonic stages of mice, we find that canonical nonhomologous end joining (NHEJ), one of the major DSB repair pathways in mammals, is predominant at 14.5 day of embryonic development. Interestingly, all four types of DSBs tested were repaired by ligase IV/XRCC4 and Ku-dependent classical NHEJ. Characterization of end-joined junctions and expression studies further showed evidences for canonical NHEJ. Strikingly, in contrast to the above, we observed noncanonical end joining accompanied by DSB resection, dependent on microhomology and ligase III in 18.5-day embryos. Interestingly, we observed an elevated expression of CtIP, MRE11, and NBS1 at this stage, suggesting that it could act as a switch between classical end joining and microhomology-mediated end joining at later stages of embryonic development. Thus, our results establish for the first time the existence of both canonical and alternative NHEJ pathways during the postimplantation stages of mammalian embryonic development.

© 2012 Elsevier Ltd. All rights reserved.

Introduction

DNA double-strand breaks (DSBs) are the most deleterious forms of DNA damage that result in a loss or rearrangement of genomic material, thereby leading to mutations, genomic instability, cancer or cell death.^{1–4} Hence, repair of DSBs is essential for maintaining genomic stability and cell viability. DSBs are induced by a number of agents and mechanisms, including exposure to ionizing radiation and radiomimetic drugs, collapse of replication forks, programmed cleavage by specific endonucleases during meiotic recombination, and immunoglobulin–TCR gene rearrangements.^{5–8} Eukaryotic cells have evolved two major pathways for repairing DSBs, namely homologous recombination (HR) and nonhomologous

*Corresponding authors. B. Choudhary is to be contacted at Institute of Bioinformatics and Applied Biotechnology, Biotech Park, Electronics City, Bangalore 560 100, India; S. Raghavan, Department of Biochemistry, Indian Institute of Science, Bangalore 560 012, India. E-mail addresses: vibha@ibab.ac.in; sathees@biochem.iisc.ernet.in.

† K.K.C. and R.S. contributed equally to this work.

Abbreviations used: DSB, double-strand break; NHEJ, nonhomologous end joining; HR, homologous recombination; MMEJ, microhomology-mediated end joining; EDTA, ethylenediaminetetraacetic acid.

end joining (NHEJ). HR has been shown to be very efficient in dividing cells and hence is most active in the S and G2 phases of the cell cycle and requires regions of extensive homology. However, NHEJ can simply rejoin a DSB with or without processing of ends and is active in all phases of the cell cycle.^{9,10}

The key players of NHEJ are a set of proteins that recognize, process, and ligate broken DNA.^{10–15} Firstly, broken DNA ends are recognized by a KU70/KU80 heterodimer, which recruits DNA-PKcs in association with Artemis.^{16–18} The DNA ends are processed by either Artemis or the DNA-PKcs–Artemis complex, such that the ends can be ligated.^{19,20} After processing, the ends are filled by Pol X family members Pol μ and Pol λ ^{21–23} and finally ligated by the XLF–XRCC4–DNA ligase IV complex.^{24–26}

Besides the classical NHEJ, recent studies have shown the existence of a microhomology-dependent alternative NHEJ within the cells. This type of joining is associated with extensive deletions, as it utilizes small homology regions.^{27,28} Although the exact mechanism remains unclear, it has been shown that alternative NHEJ is independent of KU70/KU80 heterodimer and ligase IV.^{29,30} Recent studies showed CtIP as the key protein that determines the choice between canonical NHEJ and microhomology-mediated end joining (MMEJ), favoring MMEJ in non- γ H2AX-forming DSBs.³¹ Studies also suggest that CtIP, along with MRE11 and other exonucleases, can act as an end-resecting complex to expose microhomology regions and promote MMEJ.^{30,32} This end resection is precluded by p53BP1, which is recruited and activated in a γ H2AX-dependent manner and therefore believed to be an antagonist of microhomology-mediated repair.^{33,34}

During embryonic development, DNA replication and cell proliferation occur at an increased rate. Although each component of NHEJ is required for optimal repair activity *in vitro* and is necessary for radioprotection *in vivo* (postnatal or adult stages), the expression and function of many of these genes during embryogenesis are largely unknown. The cell cycle is much shorter in embryonic cells than in adult cells.³⁵ The integrity of the genome is thus at greater risk during embryonic development, and the efficiency of DNA repair during those early stages is of great significance. Inadequately equipped oocyte or delayed zygotic gene expression is embryonically lethal.³⁶ Recently, it has been suggested that HR acts primarily during the preimplantation stages of embryonic development.³⁷ In contrast, it has been speculated that NHEJ may take over towards the later part, when cells begin to differentiate and take on specific roles.³⁸

In the present study, we show that the efficiency and mechanism of NHEJ differ in the postimplantation stages of mouse embryonic development. Cephalon at 14.5 day exhibited robust classical

NHEJ, which was further corroborated with characteristic end-joined junctions. Surprisingly, we find that 18.5-day embryos possess a noncanonical MMEJ irrespective of end configurations. Finally, we show that expression of CtIP, MRE11, and NBS1 may regulate the choice between DSB repair pathways in developing embryos.

Results

Embryos of different developmental stages exhibited varying efficiencies of DSB joining

Cell-free extracts were prepared from mice whole embryos (9.5, 12.5, and 15.5 day) or fibroblasts and cephalon (14.5, 15.5, and 18.5 day). Protein concentration and profile were normalized on SDS-PAGE (Supplementary Fig. 1a and b). Extracts were incubated with oligomeric DNA containing various DSBs with 5'–5'-compatible, 5'–5'-noncompatible, or 5'–3'-noncompatible and blunt ends, as outlined (Supplementary Fig. 2a and b). Studies using 5'-compatible termini showed that the extracts catalyzed the end-to-end joining of the substrates, resulting in dimerization and other levels of multimerization (Fig. 1a). An additional band, which we have identified as circular DNA, was seen between dimer and substrate (Fig. 1a).³⁹ The overall efficiency of end joining varied among extracts prepared from the different day points of fibroblasts, cephalon, and whole embryos (Fig. 1a and b). The 14.5-day cephalon showed maximum joining among the tissues studied (Fig. 1a, lane 4, and Fig. 1b). Among whole embryo extracts, 9.5-day extracts exhibited the weakest joining, while 12.5-day and 15.5-day extracts showed efficient joining of ends (Fig. 1a and b). Thus, studies using DSBs with compatible termini showed that extracts prepared from different stages of embryonic development were able to catalyze end joining with various efficiencies. When DSBs with blunt ends were used, the joining efficiency was much lower (Fig. 1c). However, consistent with the above studies, the overall efficiency was maximum in 14.5-day cephalon (Fig. 1c, lane 4). Non-compatible ends (5'–5' or 5'–3') also showed the most efficient joining when extracts from 14.5-day cephalon were used (Fig. 1d and e). The efficiency of joining was weaker in other cases. Thus, our data suggest that 14.5-day cephalon possess the most efficient end-to-end joining activity irrespective of the nature of termini.

NHEJ proteins express throughout the developmental stages

The presence of NHEJ proteins in the cell-free extracts of 9.5-day, 12.5-day, and 15.5-day embryos

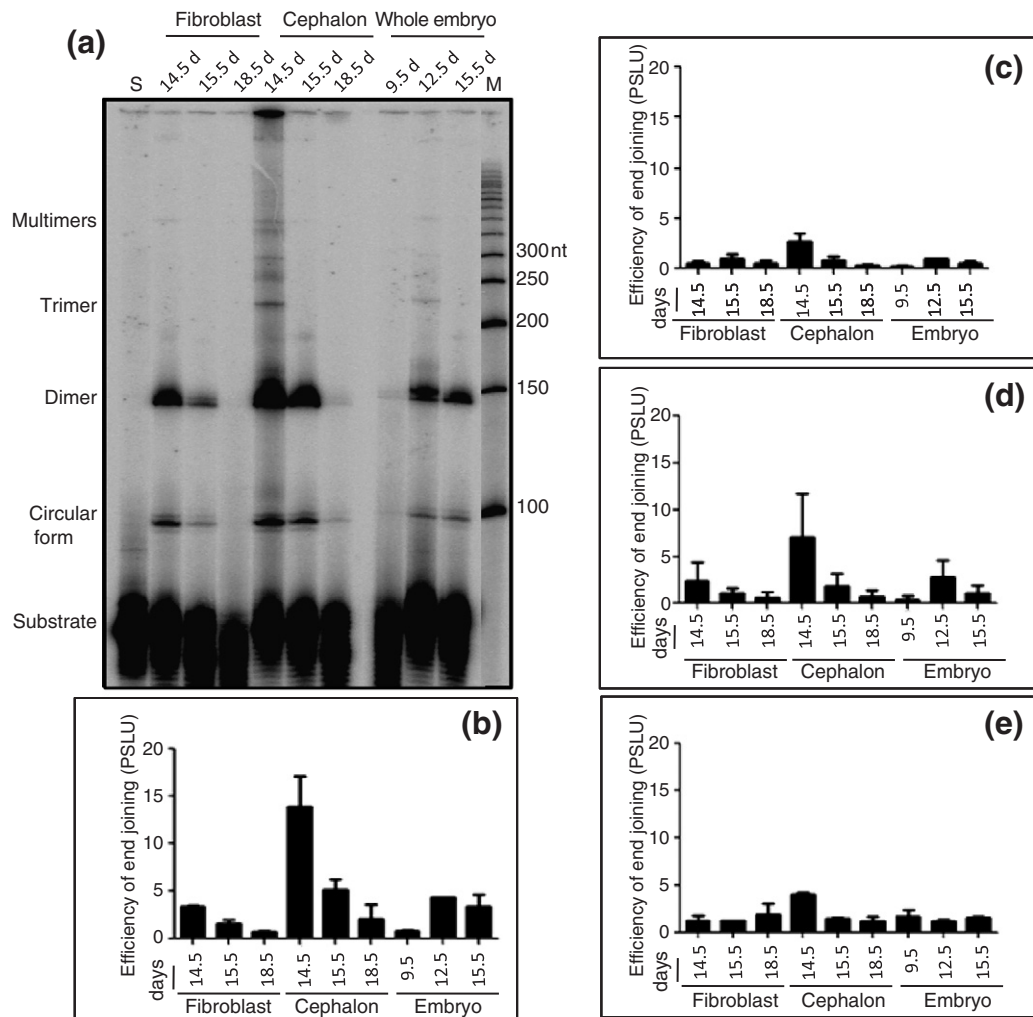


Fig. 1. Comparison of the end-joining efficiencies of different DSBs catalyzed by cell-free extracts in various developmental stages of mouse embryo. (a) Gel profile showing end-joining products resulting from DSBs with 5' overhangs. End-joining assay was performed by incubating 5 μ g of extracts with [γ - 32 P]ATP-labeled oligomeric DNA substrates at 37 $^{\circ}$ C. The reaction products were deproteinized and resolved on 8% denaturing PAGE. In the case of substrate alone, DNA was incubated in the reaction buffer and loaded (lane S). M represents a [γ - 32 P]ATP-labeled 50-bp ladder. (b–e) Bar diagram showing the quantification of end-joined products using substrates with 5'-compatible ends (b), blunt ends (c), 5'-5'-noncompatible ends, (d) and 5'-3'-noncompatible ends (e). For quantification, an area covering the DNA band of interest was selected, and the intensity was calculated and expressed as photo-stimulated luminescence (PSL) units. The same-sized rectangle was used to determine the background, which was subtracted. The intensity measured from each band in a lane, resulting from NHEJ, was added and plotted. Data represent the mean \pm standard deviation of three independent experiments.

(whole embryos) and in 14.5-day, 15.5-day, and 18.5-day embryos (fibroblasts and cephalon) was examined by Western blot analysis (Fig. 2a). Although the levels of KU70, KU80, and Pol λ were comparable among different stages, DNA-PKcs expression varied significantly (Fig. 2a and b). Expression of ligase IV was detectable in almost all stages; however, it was remarkably high in 14.5-day cephalon, which have shown the most proficient joining (Fig. 2a and b). This observation was further confirmed by immunofluorescence analysis (see the text below). XRCC4 expression was undetectable in

18.5-day cephalon, while other stages showed its robust expression (Fig. 2a).

p53 plays a central role in maintaining genomic stability by downregulating inappropriate homology-mediated genetic exchanges and by limiting the mutagenic effects of NHEJ. Our results show that p53 expression was seen throughout the development of the embryo, although its level was highest at 9.5 day (Fig. 2a and b). A similar pattern of expression was observed in the case of p73, a paralog of p53. In response to DSBs, ATM acts upstream of p53 and controls its activity through phosphorylation. Our

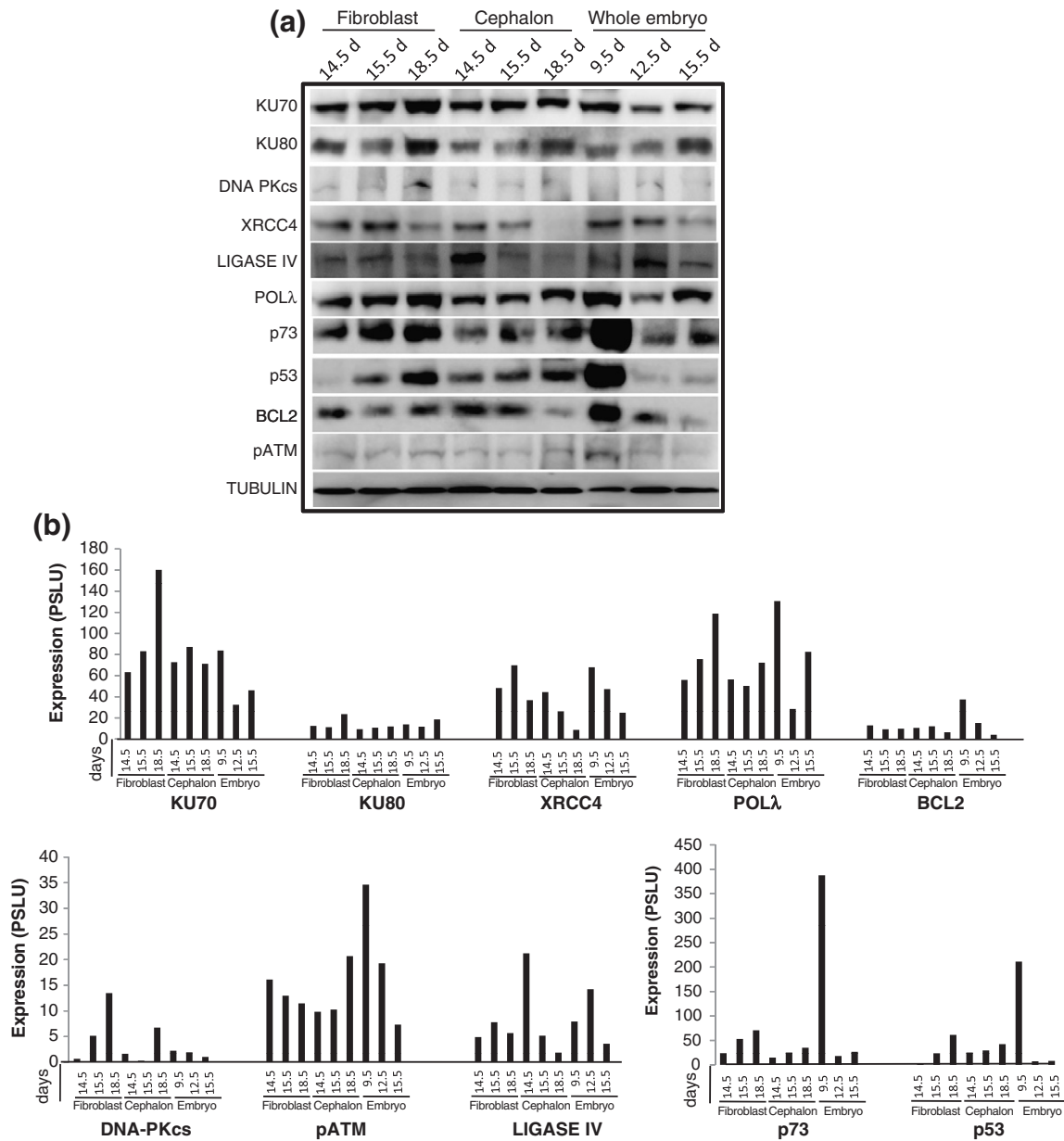


Fig. 2. Immunoblot analyses for DSB repair proteins at different stages of mouse development. (a) Expression of DSB repair proteins in mouse fibroblasts, cephalon, and whole embryos. Forty micrograms of protein lysate was resolved on SDS-PAGE and transferred to a PVDF membrane. Appropriate antibodies were used to study the expression. α -Tubulin was used as loading control. (b) Bar diagram showing the quantification of Western blot analyses shown in (a). The DNA repair proteins studied are as follows: KU70, KU80, DNA-PKcs, XRCC4, ligase IV, Pol λ , p73, p53, pATM, and BCL2. Every experiment was repeated a minimum of three independent times, with good agreement.

results show that expression of pATM was high in 9.5-day total embryos, while it was comparable in other stages. Although this could be attributed to an increased number of breaks, the significance of this observation needs to be explored (Fig. 2a and b). Furthermore, we have also checked the levels of the anti-apoptotic protein BCL2 in different developmental stages. Results showed a higher expression of BCL2 in almost all the stages, with 9.5 day being the

highest, followed by decreased expression in 12.5-day and 15.5-day whole embryos, correlating with the embryonic developmental process (Fig. 2a and b).

Immunodepletion studies suggest classical NHEJ in embryonic extracts

To reinforce the finding that the observed joining is indeed mediated by NHEJ proteins, we immuno-

precipitated the key proteins in the NHEJ pathway (KU70, KU80, and ligase IV) from the cell-free extracts of 14.5-day cephalon (Supplementary Fig. 4a–c), since that showed the maximum efficiency of joining. Immunodepletion was confirmed by Western blot analysis (Supplementary Fig. 4a–c). End-joining assay with immunodepleted extracts showed a significant reduction in joining efficiency when 5′-compatible or 5′-5′-noncompatible substrates were used (Supplementary Fig. 4d). The reduction in the efficiency was quantified relative to the controls, and data showed a significant reduction in the end-joining efficiency (Supplementary Fig. 4e and f), suggesting that the observed end joining is mediated through NHEJ. Although immunodepletion of ligase IV was not as efficient as that of KU, the depletion of ligase IV led to a remarkable reduction in NHEJ efficiency, as compared to KU70 or KU80 depletion alone. This confirms that the observed joining could be indeed mediated by ligase IV.

Sequence characteristics of NHEJ junctions

The end-joined junctions derived from different DSBs were cloned and sequenced in order to study the mechanism of joining. Since the efficiency of joining was weak in many cases, multiple joining reactions were performed, and pooled reaction products (Supplementary Fig. 5) were used as template for PCR. The products were then cloned and sequenced (Supplementary Fig. 5).

Among 10 NHEJ junctions analyzed from 5′-5′-noncompatible termini, in the case of 9.5-day whole embryos, 9 of 10 junctions showed joining with deletion of AATT overhang, while 5 of 10 showed deletion from another overhang (GATC), of which two molecules had deletions of more than 23 bp, and each had deletions of 11 and 13 bp (Fig. 3a). Most of the NHEJ junctions of 5′-3′-noncompatible ends (11 of 13) had deletions of both overhangs, of which five used microhomology for joining (Fig. 3a). Two of the clones showed joining with a deletion from one end, although insertions were rare.

We have also sequenced junctions from 53 independent clones in the case of 14.5-day embryos (Fig. 3b and c). Among these, 28 were derived from fibroblasts (Fig. 3b), while 25 were derived from cephalon (Fig. 3c). In the case of junctions resulting from the joining of 5′-5′-noncompatible and 5′-3′-noncompatible ends from 14.5-day fibroblasts, deletion from both DSBs was noted in all the clones, of which 30% used microhomology (Fig. 3b). However, insertions were absent. Interestingly, NHEJ junctions derived from blunt ends of 14.5-day fibroblasts also resulted in the deletion of nucleotides from both sides of DSB, of which 50% of the molecules showed insertions of 8 nt each (Fig. 3b). In the case of 25 NHEJ junctions studied from

14.5-day cephalon, 9 showed microhomology-mediated joining. DSBs with 5′-5′-noncompatible ends showed deletions in all 12 clones sequenced, of which one had longer deletions (18 and 29 bp each from the left and the right) (Fig. 3c). Four of 12 molecules had independent insertions. Interestingly, none of the clones showed insertion in junctions resulting from 5′-3′ overhangs, although deletions were frequent (Fig. 3c). Similar results were observed when DSBs with blunt ends were studied.

One hundred twenty-one independent NHEJ junctions derived from all four different DSBs were studied in the case of 18.5-day embryos. To our surprise, we found that, irrespective of termini, in 18.5-day embryos, the majority (107 of 121; 88%) of joining used microhomology (Fig. 3d and e). Interestingly, among them, 77% molecules had 3-nt microhomology (GCC)-associated joining. Stretches of nucleotides were deleted from both ends until the microhomology region was exposed (Fig. 3d and e). In the case of NHEJ junctions of 5′-5′-noncompatible ends derived from 18.5-day fibroblasts and cephalon, joining was associated with deletions in all the clones (25 of 25) (Fig. 3d and e); of that, 24 of 25 and 19 of 25 molecules showed microhomology-mediated joining in fibroblasts and cephalon, respectively. Since 18.5-day fibroblasts and cephalon showed microhomology-mediated joining in the case of noncompatible and blunt ends, we also tested the joining mechanism with compatible ends. Junctions from clones obtained were digested with BamHI to remove those joined by simple ligation. Sequence analysis showed that 3-nt microhomology was used for joining in most of the cases (Fig. 3d). Hence, characterization of NHEJ junctions from 18.5-day embryos demonstrated that, in most of the cases, nucleotides were deleted from both termini until the microhomology region was exposed, and then the two ends were ligated.

18.5-Day embryos possess efficient microhomology-mediated joining

Since high levels of microhomology usage were observed in 18.5-day extracts, we wondered how efficiently the extract can carry out end joining if microhomology-containing substrates were provided (Fig. 4a). Two independent oligomeric DNA substrates (SS69/70 and SS71/72) possessing 13-nt microhomology were incubated with the respective cell extracts, and the joined products were detected by radioactive PCR (Fig. 4a and b; Supplementary Table 1). Fibroblasts at 14.5 day were taken as control, as they used microhomology only in limited cases. Interestingly, a 63-nt band was seen in the case of 18.5-day cephalon (arrow) due to microhomology-associated joining, whereas the band was much weaker in the case of 18.5-day fibroblasts (Fig. 4b).

(a)				(c)			
9.5 d total embryo				14.5 d cephalon			
Deleted sequences Number of				Deleted sequences Number of			
5'-5' noncompatible ends				5'-3' non compatible ends			
5' ... AGTCTAGCCTGAG (AATT)	GATC	CCTCTAGATATCGGGCCCTC.3'	04 00 04/10	5' ... AGTCTAGCCTGAG (GATC) CCTCTAGATATCGGGCCCTC.3'	04 13 02/06		
5' ... AGTCTAGCCTGAG (AATT)	(GATC)	CCTCTAGATATCGGGCCCTC.3'	04 23 02/10	5' ... AGTCTAGCCTGAG (GATC) CCTCTAGATATCGGGCCCTC.3'	04 00 01/06		
5' ... AGTCTAGCCTGAG (AATT)	(GATC)	CCTCTAGATATCGGGCCCTC.3'	03 11 01/10	5' ... AGTCTAGCCTGAG (GATC) CCTCTAGATATCGGGCCCTC.3'	06 11 01/06		
5' ... AGTCTAGCCTGAG (AATT)	(GATC)	CCTCTAGATATCGGGCCCTC.3'	08 13 01/10	5' ... AGTCTAGCCTGAG (GATC) CCTCTAGATATCGGGCCCTC.3'	04 05 01/06		
5' ... AGTCTAGCCTGAG (AATT)	GATC	CCTCTAGATATCGGGCCCTC.3'	04 01 01/10	5' ... AGTCTAGCCTGAG (GATC) CCTCTAGATATCGGGCCCTC.3'	00 00 01/06		
5' ... AGTCTAGCCTGAG (AATT)	(GATC)	CCTCTAGATATCGGGCCCTC.3'	13 04 01/10				
5'-3' noncompatible ends				Blunt ends			
5' ... AGTCTAGCCTGAG	GATC	CCTCTAGATATCGGGCCCTC.3'	09 00 02/13	5' ... AGTCTAGCCTGGCCC	GGGCTCTAGATATCGGGCCCTC.3'	00 00 01/07	
5' ... AGTCTAGCCTGAG	(GATC)	CCTCTAGATATCGGGCCCTC.3'	03 07 02/13	5' ... AGTCTAGCCTGGCCC	GGGCTCTAGATATCGGGCCCTC.3'	00 08 02/07	
5' ... AGTCTAGCCTGAG	(GATC)	CCTCTAGATATCGGGCCCTC.3'	04 13 04/13	5' ... AGTCTAGCCTGGCCC	GGGCTCTAGATATCGGGCCCTC.3'	06 03 01/07	
5' ... AGTCTAGCCTGAG	(GATC)	CCTCTAGATATCGGGCCCTC.3'	05 04 01/13	5' ... AGTCTAGCCTGGCCC	GGGCTCTAGATATCGGGCCCTC.3'	00 08 01/07	
5' ... AGTCTAGCCTGAG	(GATC)	CCTCTAGATATCGGGCCCTC.3'	03 23 01/13	5' ... AGTCTAGCCTGGCCC	GGGCTCTAGATATCGGGCCCTC.3'	06 11 01/07	
5' ... AGTCTAGCCTGAG	(GATC)	CCTCTAGATATCGGGCCCTC.3'	04 18 01/13	5' ... AGTCTAGCCTGGCCC	GGGCTCTAGATATCGGGCCCTC.3'	06 09 01/07	
5' ... AGTCTAGCCTGAG	(GATC)	CCTCTAGATATCGGGCCCTC.3'	04 21 01/13	5' ... AGTCTAGCCTGGCCC	GGGCTCTAGATATCGGGCCCTC.3'	06 09 01/07	
5' ... AGTCTAGCCTGAG	GCCC (GATC)	CCTCTAGATATCGGGCCCTC.3'	02 10 01/13				
(b)				(d)			
14.5 d fibroblasts				18.5 d fibroblast			
5'-5' noncompatible ends				Blunt ends			
5' ... AGTCTAGCCTGAG (AATT)	(GATC)	CCTCTAGATATCGGGCCCTC.3'	11 18 02/11	5' ... AGTCTAGCCTGGCCC	GGGCTCTAGATATCGGGCCCTC.3'	06 19 12/17	
5' ... AGTCTAGCCTGAG (AATT)	(GATC)	CCTCTAGATATCGGGCCCTC.3'	03 11 02/11	5' ... AGTCTAGCCTGGCCC	GGGCTCTAGATATCGGGCCCTC.3'	06 16 02/17	
5' ... AGTCTAGCCTGAG (AATT)	(GATC)	CCTCTAGATATCGGGCCCTC.3'	11 09 01/11	5' ... AGTCTAGCCTGGCCC	GGGCTCTAGATATCGGGCCCTC.3'	05 22 01/17	
5' ... AGTCTAGCCTGAG (AATT)	(GATC)	CCTCTAGATATCGGGCCCTC.3'	12 07 01/11	5' ... AGTCTAGCCTGGCCC	GGGCTCTAGATATCGGGCCCTC.3'	06 03 01/17	
5' ... AGTCTAGCCTGAG (AATT)	(GATC)	CCTCTAGATATCGGGCCCTC.3'	08 21 01/11	5' ... AGTCTAGCCTGGCCC	GGGCTCTAGATATCGGGCCCTC.3'	10 01 01/17	
5' ... AGTCTAGCCTGAG (AATT)	(GATC)	CCTCTAGATATCGGGCCCTC.3'	08 18 01/11				
5' ... AGTCTAGCCTGAG (AATT)	(GATC)	CCTCTAGATATCGGGCCCTC.3'	08 13 01/11	5'-5' noncompatible ends			
5' ... AGTCTAGCCTGAG (AATT)	(GATC)	CCTCTAGATATCGGGCCCTC.3'	04 11 01/11	5' ... AGTCTAGCCTGAG (AATT)	(GATC) CCTCTAGATATCGGGCCCTC.3'	08 21 21/25	
5' ... AGTCTAGCCTGAG (AATT)	GATC	CCTCTAGATATCGGGCCCTC.3'	04 00 01/11	5' ... AGTCTAGCCTGAG (AATT)	(GATC) CCTCTAGATATCGGGCCCTC.3'	10 11 02/25	
5'-3' noncompatible ends				5' ... AGTCTAGCCTGAG (AATT)	(GATC) CCTCTAGATATCGGGCCCTC.3'	05 18 01/25	
5' ... AGTCTAGCCTGAG	(GATC)	CCTCTAGATATCGGGCCCTC.3'	06 19 04/07	5' ... AGTCTAGCCTGAG (AATT)	(GATC) CCTCTAGATATCGGGCCCTC.3'	04 11 01/25	
5' ... AGTCTAGCCTGAG	(GATC)	CCTCTAGATATCGGGCCCTC.3'	06 23 01/07				
5' ... AGTCTAGCCTGAG	(GATC)	CCTCTAGATATCGGGCCCTC.3'	03 07 01/07	5'-3' noncompatible ends			
5' ... AGTCTAGCCTGAG	(GATC)	CCTCTAGATATCGGGCCCTC.3'	09 11 01/07	5' ... AGTCTAGCCTGAG (AATT)	(GATC) CCTCTAGATATCGGGCCCTC.3'	04 21 16/19	
Blunt ends				5' ... AGTCTAGCCTGAG (AATT)	(GATC) CCTCTAGATATCGGGCCCTC.3'	12 10 01/19	
5' ... AGTCTAGCCTGGCCC	GAGGATCC	GGGCTCTAGATATCGGGCCCTC.3'	05 03 04/10	5' ... AGTCTAGCCTGAG (AATT)	(GATC) CCTCTAGATATCGGGCCCTC.3'	01 18 01/19	
5' ... AGTCTAGCCTGGCCC		GGGCTCTAGATATCGGGCCCTC.3'	00 08 03/10	5' ... AGTCTAGCCTGAG (AATT)	(GATC) CCTCTAGATATCGGGCCCTC.3'	04 05 01/19	
5' ... AGTCTAGCCTGGCCC	AT	GGGCTCTAGATATCGGGCCCTC.3'	06 04 01/10				
5' ... AGTCTAGCCTGGCCC	GAGGATCC	GGGCTCTAGATATCGGGCCCTC.3'	00 03 01/10	5'-5' compatible ends			
5' ... AGTCTAGCCTGGCCC		GGGCTCTAGATATCGGGCCCTC.3'	05 19 01/10	5' ... AGTCTAGCCTGAG (AATT)	(GATC) CCTCTAGATATCGGGCCCTC.3'	08 21 15/22	
				5' ... AGTCTAGCCTGAG (AATT)	(GATC) CCTCTAGATATCGGGCCCTC.3'	08 05 04/22	
				5' ... AGTCTAGCCTGAG (AATT)	GATC CCTCTAGATATCGGGCCCTC.3'	04 00 02/22	
				5' ... AGTCTAGCCTGAG (AATT)	TTCAGGCC CCTCTAGATATCGGGCCCTC.3'	16 15 01/22	
					TCTAGATCC		
(e)				(e)			
14.5 d cephalon				18.5 d Cephalon			
5'-5' non compatible ends				5'-5' noncompatible ends			
5' ... AGTCTAGCCTGAG (GATC) CCTCTAGATATCGGGCCCTC.3'	00 11 02/12			5' ... AGTCTAGCCTGAG (AATT)	(GATC) CCTCTAGATATCGGGCCCTC.3'	08 21 18/25	
5' ... AGTCTAGCCTGAG (GATC) CCTCTAGATATCGGGCCCTC.3'	00 11 01/12			5' ... AGTCTAGCCTGAG (AATT)	(GATC) CCTCTAGATATCGGGCCCTC.3'	08 05 06/25	
5' ... AGTCTAGCCTGAG (GATC) CCTCTAGATATCGGGCCCTC.3'	00 11 01/12			5' ... AGTCTAGCCTGAG (AATT)	(GATC) CCTCTAGATATCGGGCCCTC.3'	08 24 01/25	
5' ... AGTCTAGCCTGAG (GATC) CCTCTAGATATCGGGCCCTC.3'	01 11 01/12						
5' ... AGTCTAGCCTGAG (GATC) CCTCTAGATATCGGGCCCTC.3'	03 11 01/12			Blunt ends			
5' ... AGTCTAGCCTGAG (GATC) CCTCTAGATATCGGGCCCTC.3'	06 11 01/12			5' ... AGTCTAGCCTGGCCC	GGGCTCTAGATATCGGGCCCTC.3'	06 20 09/13	
5' ... AGTCTAGCCTGAG (GATC) CCTCTAGATATCGGGCCCTC.3'	00 09 01/12			5' ... AGTCTAGCCTGGCCC	GGGCTCTAGATATCGGGCCCTC.3'	06 03 01/13	
5' ... AGTCTAGCCTGAG (GATC) CCTCTAGATATCGGGCCCTC.3'	09 00 01/12			5' ... AGTCTAGCCTGGCCC	GGGCTCTAGATATCGGGCCCTC.3'	06 00 01/13	
5' ... AGTCTAGCCTGAG (GATC) CCTCTAGATATCGGGCCCTC.3'	03 07 01/12			5' ... AGTCTAGCCTGGCCC	GGGCTCTAGATATCGGGCCCTC.3'	00 06 01/13	
5' ... AGTCTAGCCTGAG (GATC) CCTCTAGATATCGGGCCCTC.3'	18 29 01/12			5' ... AGTCTAGCCTGGCCC	GGGCTCTAGATATCGGGCCCTC.3'	00 13 01/13	

Fig. 3. Sequence analysis of NHEJ junctions. DNA sequences at the joining junctions of NHEJ derived from 9.5-day whole embryos (a), 14.5-day fibroblasts (b), 14.5-day cephalon (c), 18.5-day fibroblasts (d), and 18.5-day cephalon (e). Deleted nucleotides are denoted in red, and deletion of overhang is presented in red parentheses. The nucleotides in blue represent insertions at the junction, and the microhomology region is underlined. All NHEJ junctions shown are derived from either independent junctions of the same molecules or different clones derived from independent PCR and transformations.

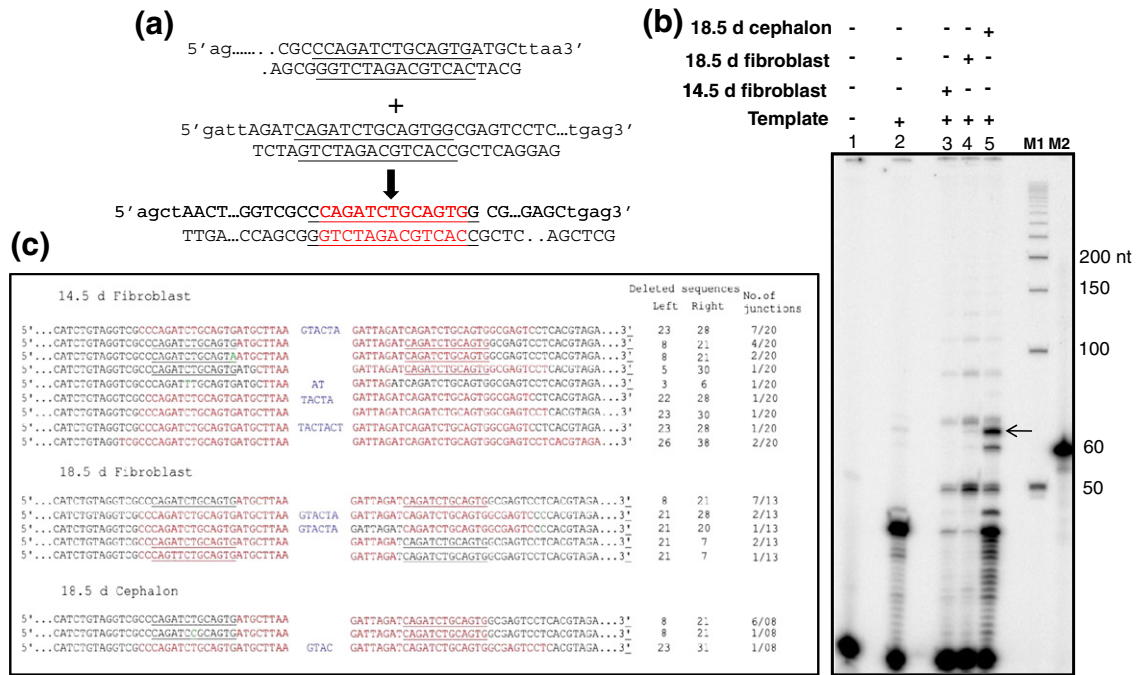


Fig. 4. Efficiency of MMEJ and sequence analysis of junctions derived from microhomology-containing substrates. (a) Schematic presentation of the 13-nt microhomology substrate used and the expected reaction products. The region of microhomology is underlined in the substrates, while the end-joined region containing microhomology is shown in red and underlined. (b) PAGE profile showing microhomology-mediated joining following PCR amplification using radiolabeled primers. The arrow indicates the expected 63-nt-long dimeric product resulting from microhomology-mediated joining (lane 5). Other bands in lanes 3–5 could be the result of microhomology-independent NHEJ products. The presence of bands in no-protein lane (lane 2) could be due to nonspecific primer extension. M1 and M2 indicate a 50-bp molecular mass ladder and a 60-nt marker, respectively. (c) DNA sequences at the joining junctions of NHEJ products derived from 14.5-day fibroblasts, 18.5-day fibroblasts, and 18.5-day cephalon when microhomology-containing substrates were used. Deleted nucleotides are denoted in red. The nucleotides in blue represent insertions at the junction, and the microhomology region is underlined. All the NHEJ junctions shown are derived from either independent junctions of the same molecules or different clones derived from independent PCR and transformations.

Bands due to canonical end joining were also seen (Fig. 4b).

Cloning and sequencing of end-joined junctions showed that, in the case of 18.5-day fibroblasts, 7 of 13 junctions analyzed utilized 13-nt microhomology (Fig. 4c). In other cases, deletions with insertions and deletions alone were seen with 3 junctions each. Interestingly, 18.5-day cephalon showed maximum homology-mediated joining, as 7 of 8 junctions joined through 13-nt microhomology (Fig. 4c). Taken together, results from this study and the above studies suggest extensive microhomology usage for joining in 18.5-day embryos (Fig. 4). In the case of 14.5-day fibroblasts, 7 of the 20 junctions analyzed used microhomology for joining (Fig. 4c). The rest of the junctions showed classical NHEJ-mediated joining with insertions (10 of 20) or deletions (3 of 10). Interestingly, the fraction of the total junctions that used microhomology for joining (7 of 20) was comparable to an earlier sequence analysis (compare Figs. 3 and 4). This suggests that the experimental systems used in the present study

reflect the innate ability of extracts to carry out DNA end joining using different mechanisms.

MMEJ-associated proteins exhibit a unique expression pattern in 18.5-day embryos

Since we found elevated levels of microhomology-mediated joining in 18.5-day extracts, we tested whether the expression of MMEJ proteins correlates with the observed joining. Interestingly, Western blot analysis showed an elevated expression of CtIP, MRE11, NBS1, and ligase III in 18.5-day embryonic extracts (whether fibroblasts or cephalon) compared to the 14.5-day and 15.5-day embryonic extracts analyzed (Fig. 5a). A similar expression pattern was also observed for cell-cycle-regulated proteins such as cyclins B1 and D1, suggesting a link between cell cycle regulation and CtIP expression, as seen earlier.^{40,41} Among fibroblasts and cephalon, the fibroblasts were found to have a higher expression of CtIP, MRE11, NBS1, and ligase III. However, we could not find any

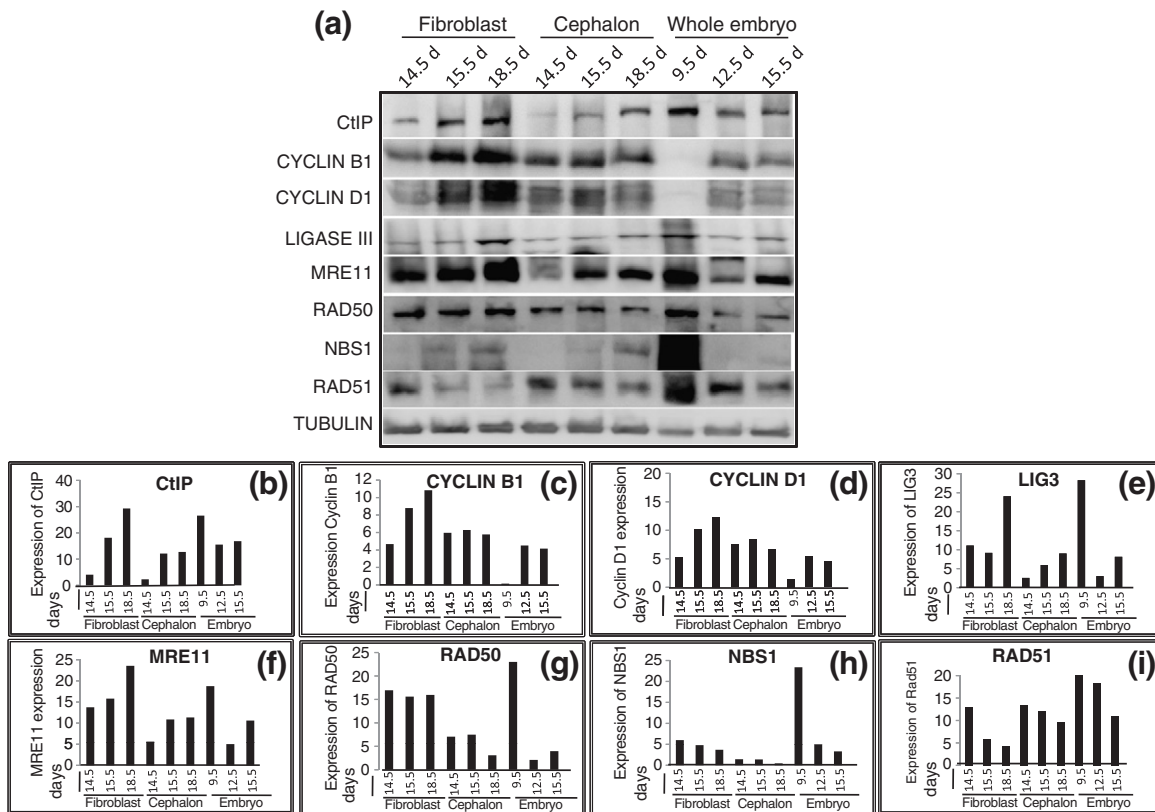


Fig. 5. Immunoblot analysis of MMEJ-associated proteins at different stages of mouse development. (a) Blots showing the expression of MMEJ-associated proteins in mouse fibroblasts, cephalon, and whole embryos. α -Tubulin was used as loading control. (b) Bar diagram showing the quantification of Western blot analyses shown in (a). The DNA repair proteins studied are as follows: (b) CtIP, (c) cyclin B1, (d) cyclin D, (e) ligase III, (f) MRE11, (g) RAD50, (h) NBS1, and (i) RAD51. Each Western blot analysis shown was repeated a minimum of three independent times, with consensus.

significant difference in the expressions of RAD50 between the different stages analyzed (Fig. 5a and b). Similarly, 9.5-day whole embryos also showed a higher expression of CtIP, MRE11, NBS1, and RAD50 (Fig. 5a and b). Besides, we observed an elevated expression of RAD51 in 9.5-day whole embryos (Fig. 5a and b), indicating that HR could be the DNA repair pathway in early embryonic stages, consistent with a previous report.³⁷

MMEJ proteins show maximum expression at 18.5 day *in vivo* and are inversely proportional to p53BP1 level

Since the expression of MMEJ-associated proteins was highest in the cell-free extracts of 18.5-day embryos, we tested their spatial expression among tissues of different developmental stages *in situ*. Immunofluorescence analysis on cross sections of 14.5-day and 18.5-day fibroblasts and brain for CtIP, MRE11, ligase III, and p53BP1 (Fig. 6a, c, and d) showed that CtIP was expressed in 18.5-day fibroblasts and brain; the fibroblasts

showed a relatively higher expression than the brain, consistent with immunoblotting analysis (Fig. 6a, b and d; Supplementary Fig. 6a–e). In the fibroblasts and brain sections of 14.5-day embryos, the protein was largely distributed along the epidermal layer and proliferating follicles (Fig. 6a, a and c). Ligase III also showed maximum expression in 18.5-day fibroblasts compared to 14.5-day fibroblasts (Fig. 6d, a and b), while the expression level and pattern were largely comparable among 14.5-day and 18.5-day cephalon (Fig. 6d, c and d). Comparable results were obtained when MRE11 expression was studied and exhibited maximum expression in 18.5-day fibroblasts (Fig. 6c, a and b). Among the different stages of the brain studied, there was a higher expression of MRE11 at 18.5 day, mainly at the periphery of the tissues (Fig. 6c, c and d). In contrast, we observed that ligase IV expression in the brain was maximum at 14.5 day, compared to the other stages studied (Fig. 6e). These observations suggest that proteins implicated to have a role in MMEJ showed the highest expression in rapidly proliferating tissues such as the fibroblasts,

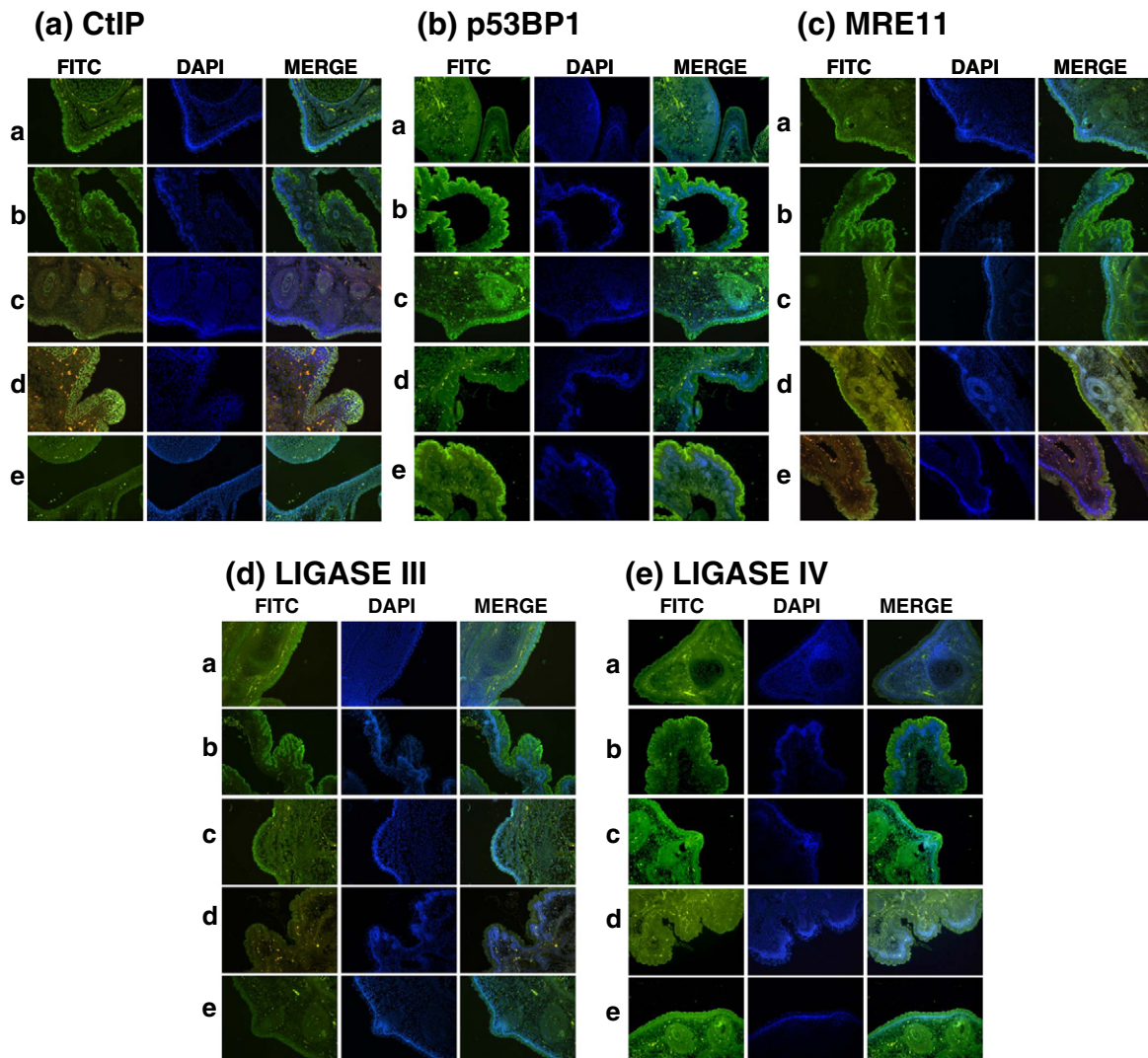


Fig. 6. Immunofluorescence analysis of selected MMEJ and NHEJ proteins in tissues of different mouse developmental stages. Immunofluorescence staining for CtIP (a), p53BP1 (b), MRE11 (c), ligase III (d), and ligase IV (e) in 14.5-day fibroblasts (a), 18.5-day fibroblasts (b), 14.5-day cephalon (c), and 18.5-day cephalon (d). Immunofluorescence staining was carried out using the respective antibodies and fluorescein-isothiocyanate-conjugated secondary antibody. Images were taken at a magnification of 10 \times . Controls indicate secondary antibody alone (e). The basal level of fluorescence in controls is due to the autofluorescence of the tissues. A 9.5-day embryo was not analyzed because of high autofluorescence. The experiment was performed a minimum of three independent times, and representative images are presented.

and that the levels of expression attained their peak towards the end phase of gestation (18.5 day). We have also tested for DSB foci formation by using p53BP1 staining. Results showed efficient foci formation in 14.5-day cephalon confined to distinct areas in the epidermis; however, the levels decreased as gestation period increased (Fig. 6b). It is interesting to note that, based on our observations, p53BP1 levels were directly correlated to NHEJ efficiency and inversely related to MMEJ efficiency at the postimplantation stages of embryonic development.

Discussion

Maintaining genomic integrity during embryonic development is of great significance to an organism, as cells tend to divide much faster. Mammalian cells have developed complex mechanisms to identify DNA damage and to activate the responses required to maintain genome integrity. When a fertilized egg develops into an embryo, it acquires a greater ability to respond to DNA damage by regulating/reprogramming DNA repair genes. The expression patterns of DNA damage response genes may determine

developmental repair status and susceptibility to genotoxic stress during organogenesis.

Why use a cell-free system to study DSB repair in embryos?

Among different methods for studying DSB repair, we chose a cell-free repair system that essentially contains all cellular proteins isolated by ammonium sulfate precipitation, since studying end joining *in vivo* is not possible during the different developmental stages of an embryo. Oligomeric DNA containing different types of DSBs, including noncompatible termini, which can mimic *in vivo* DSBs, were used to assess various modes of end joining. It is well accepted that results obtained in such assays broadly match the repair activity within the cells. In fact, such cell-free assay systems were used previously to provide new insights into NHEJ in various model systems.^{42–46} Besides the efficiency of repair, the mechanism of regulation of NHEJ, the regulation of their proteins, and various protein–protein interactions were also studied using such a system.^{15,39,43–45,47–54} However, it is not clear whether the end-joining events observed in our studies correspond to *in vivo* NHEJ events, although the various lines of experimental evidence suggest an *in vivo* mechanistic correlation. Moreover, we could also correlate the expression of proteins detected by immunoblotting at different developmental stages to the immunofluorescence observed at the intracellular level (see the text below).

14.5-Day cephalon possess robust NHEJ activity

Using this oligomer-based cell-free DSB repair system in which joining of different DSBs could mimic *in vivo* repair, we found that cell-free extracts prepared from various stages of embryo development catalyzed intermolecular joining, resulting in dimers, trimers, tetramers, and multimers. Majority of the joined products observed by us were consistent with those shown in earlier reports.^{15,39,50,53,54} In contrast to some of the earlier reports, we also observed intramolecular circularization.^{42,53–55}

Comparison of NHEJ activities showed that the joining of DSBs was highest in 14.5-day cephalon, irrespective of the nature of DSBs. Consistent with this, immunofluorescence studies using p53BP1 also showed the highest levels of innate DSBs within the cells at this stage, justifying the need for an efficient NHEJ system. The observed pattern of joining was comparable to the one reported for mice testicular extracts.^{44,48} The higher efficiency of joining for compatible ends in different extracts is understand-

able, as these ends could be ligated with or without further modification (Fig. 3).^{39,48,54} Previous studies also suggest that complementary cohesive ends can be rejoined in an error-free manner by precise ligation and may require only some components such as KU proteins and the XRCC4–ligase IV complex of the NHEJ pathway.⁵⁶ In contrast, rejoining of noncompatible DNA ends requires end processing and thus additional factors such as Artemis, DNA–PKcs, and the polymerase activities of Pol μ and Pol λ .^{23,56,57} DNA ends with noncomplementary 3' overhangs present the most complex problem for the NHEJ machinery. Unlike 5' overhangs, 3' overhangs cannot be filled in without external priming, and if the other 3' overhang in the reaction is not complementary, it is not immediately evident how such priming could occur. Hence, repair by NHEJ can be an error-free process or an error-prone process, determined in part by different types of DNA ends.

Restriction digestion analysis, in conjunction with DNA sequencing studies, showed that the compatible ends were joined mostly without end processing, except in the case of 18.5-day fibroblasts (Fig. 3; data not shown). In the case of noncompatible ends, joining was more complicated and required end modifications at different levels, consistent with earlier studies.^{51,58,59} Generally, end processing includes exonuclease/endonuclease resection of ends, gap filling, and ligation by NHEJ proteins.⁵ Sequence analysis of joined junctions from noncompatible and blunt-end termini showed the presence of processed ends, DNA synthesis, and extended deletions, indicating that the joining utilized NHEJ. Junctional sequence analysis of 5'–5'/5'–3'-noncompatible and blunt-end termini in all cases revealed deletion of the nucleotides of one or both overhangs, as well as those from both sides of the junctions, indicating nucleotide loss followed by blunt-end ligation. This could be due to the action of a dominant unregulated processive nuclease.⁴⁶

We found that the efficiency of NHEJ pathways among developmental stages was largely comparable to the expression of NHEJ proteins. Immunoblotting and immunofluorescence analyses further confirmed the same. Specifically, the highest ligase IV expression in 14.5-day cephalon could be correlated with the observed elevated NHEJ. Consistent with this, the expression of XRCC4 was also high at this developmental stage. The observed higher expression of HR proteins at 9.5 days is consistent with a previous report where elevated HR has been suggested during early embryonic development.³⁷

18.5-Day embryos predominantly use microhomology-dependent NHEJ activity

Although the literature has described multiple mechanisms of DSB repair to process different types

of DSBs, we observed a predominant noncanonical mechanism of NHEJ in 18.5-day embryos (Fig. 7a and b). This mechanism was dependent on microhomology and used a 3-nt to 13-nt microhomology region for the joining of DSBs (Fig. 4). It appears that, during the joining, the microhomology region was exposed by exonuclease action, followed by processing of the flap region, finally resulting in the ligation of processed ends. Such microhomology-mediated joining has been described in mammalian cells by various groups.^{51,55,59} Invariably, this mechanism might result in the loss of some original DNA sequence, irrespective of the nature of DSBs. However, it helps in maintaining the integrity of the genome. *Xenopus* egg extracts have previously been recognized to rarely use this mechanism, possibly because of low nuclease activity and/or large amounts of end-protecting Ku protein.^{47,53,60} However, unlike other systems, we noted that >77% of the joining catalyzed by 18.5-day embryos was microhomology dependent (Fig. 7).

Proliferation is highest towards the second half of embryonic development; hence, division-induced chromosomal breaks also reach maximum.⁶¹ It has been reported that proteins such as DDB1 (UV-damaged DNA binding protein 1) express maximally during the active proliferative stage and are distributed in the periphery of the epidermis.⁶¹ Interestingly, MMEJ-associated proteins such as CtIP, MRE11, NBS1, and ligase III also showed their highest expression in differentiating and actively proliferating tissues. The observed elevated

CtIP expression can also be correlated to the cell cycle regulatory proteins, cyclins.

Furthermore, we observed that p53BP1, an antagonist of the MMEJ pathway, expressed maximally in 14.5-day cephalon and expressed the least in 18.5-day embryos (Fig. 6).^{33,34} These expression levels were directly and inversely proportional to the NHEJ and MMEJ efficiencies observed in the cell-free extracts of 14.5-day and 18.5-day embryos, respectively. Therefore, it appears that p53BP1 plays a role in shifting the pathway from NHEJ to MMEJ by its differential expression as gestation progresses. In accordance with this, we also find a concomitant switch in the expression of classical NHEJ proteins and proteins implicated in a nonclassical NHEJ pathway. For example, we find an elevated expression of classical NHEJ proteins, such as ligase IV and XRCC4, at 14.5 days of embryonic development, especially in cephalon, in which natural DSBs were at maximum (Fig. 2).^{15,62} Furthermore, the observed stage-dependent upregulation of CtIP both *in vitro* and *in vivo*, along with the MRN complex at the translational level, is of interest especially at 18.5 days, as this stage showed the maximum amount of microhomology-dependent joining. Recently, it has been suggested that CtIP, in conjunction with MRE11, might act as a switch between classical and nonclassical NHEJ.^{31,32,63} To our surprise, we found that the expression of both MRE11 and NBS1 was also higher at 18.5 days of development (Fig. 5). A similarly increased expression of ligase III at 18.5 days further justifies the predominant

(a)

Substrate	No microhomology		13 nt microhomology	
	NHEJ (%)	MMEJ (%)	NHEJ (%)	MMEJ (%)
9.5 d total embryo	70	30	na	na
14.5 d fibroblasts	61	39	65	35
14.5 d cephalon	84	16	na	na
18.5 d fibroblasts	12	88	23	77
18.5 d cephalon	11	89	12	88

(b)

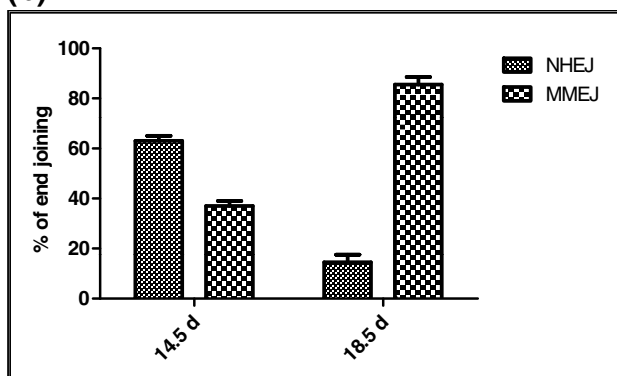


Fig. 7. Summary of the mechanism of DNA end joining at different developmental stages of mouse embryonic development. (a) Comparison of NHEJ and MMEJ junctions. Sequence analysis representing the percentage of molecules joined, using either NHEJ (derived from DSBs with blunt, 5'-5'-noncompatible, and 5'-3'-noncompatible termini) or MMEJ, with substrates containing no microhomology or limited microhomology and 13-nt microhomology. "na" indicates not assayed. (b) Graphical representation of the percentage of total junctions that followed NHEJ or MMEJ in 14.5-day and 18.5-day extracts. Error bars indicate the percentage difference in NHEJ or MMEJ between experiments carried out using substrates with dedicated microhomology and experiments carried out using substrates without dedicated microhomology.

MMEJ at 18.5 days.^{64,65} This also implies that ligase III can function as a back-up ligase when the efficiency of canonical NHEJ is low. Thus, modulation of the expression of nonclassical NHEJ proteins might play a critical role in determining the different DSB repair pathways in developing embryos.

Hence, in the present study, we establish the interplay of canonical end joining and alternative end joining during the second half of embryonic development. Previously, it has been shown that HR is predominant during the early stages of embryonic development. The observed upregulation of CtIP, MRN complex, and RAD51 in 9.5-day embryos in our studies provides compelling evidence for the occurrence of HR during the first half of embryonic development.

Thus, our study provides new insights into DSB repair during the second half of embryonic development. The observed higher levels of MMEJ are interesting, considering that they are at the final stages of development (18.5 day) and that NHEJ is predominant to HR in adult mice. Reflecting these observations, we suggest that the predominant DSB repair pathways could be different at different prenatal developmental stages, commencing with HR at the inception, followed by NHEJ and, later, by MMEJ towards the end phase of gestation. However, the implications of having MMEJ during embryonic development need to be investigated further.

Materials and Methods

Reagents, enzymes, and chemicals

All chemical reagents were obtained from Sigma Chemical Co. (USA), Amresco (USA), and SRL (India). DNA-modifying enzymes were obtained from New England Biolaboratories (USA), and antibodies were obtained from Santa Cruz Biotechnology (USA). Radioisotope-labeled nucleotides were obtained from BRIT (India).

Preparation of the cell-free extracts of mouse embryos at different developmental stages

Balb/c mice, housed in a pathogen-free facility, were mated at a male/female ratio of 1:3 and checked for vaginal plugs. Embryos were obtained at 9.5, 12.5, 14.5, 15.5, and 18.5 days. Whole embryos were dissected, and fibroblasts and cephalon were collected by removing uterine horns from 14.5-day, 15.5-day, and 18.5-day embryos. [Since the number of cells was too small during the early developing stages (9.5 and 12.5 days), whole embryos were used in preparing the extracts.] Tissues were cleared off blood by washing in ice-cold phosphate-buffered saline and stored at -80°C until use. Cell-free extracts were prepared as described earlier.^{44,54} In brief, tissues were minced to generate a single-cell suspension, resuspended in buffer A [10 mM Tris-HCl (pH 8.0), 1 mM ethylenediaminetetraacetic acid (EDTA), 5 mM DTT, and

0.5 mM PMSF] with protease inhibitors (1 $\mu\text{g}/\text{ml}$ each of leupeptin, chymostatin, and pepstatin), and homogenized. An equal volume of buffer B [50 mM Tris-HCl (pH 8.0), 10 mM MgCl_2 , 2 mM DTT, 0.5 mM PMSF, 25% sucrose, and 50% glycerol] was added, followed by the addition of saturated ammonium sulfate solution (11% cutoff), with stirring (30 min), and the supernatant was collected after centrifugation (for 3 h at 32,000 rpm and 2°C). Proteins precipitated with ammonium sulfate (65%) were pelleted and dissolved in buffer C [25 mM HEPES-KOH (pH 7.9), 0.1 M KCl, 12 mM MgCl_2 , 1 mM EDTA, 2 mM DTT, and 17% glycerol] and dialyzed for 16 h. Extracts were aliquoted and stored at -80°C until use. Protein concentration was determined by Bradford assay. The amount of protein was normalized further by loading on SDS-PAGE, followed by staining with Coomassie brilliant blue (Supplementary Fig. 1a and b).

Preparation of DNA substrates for NHEJ

Oligomers were gel purified, and [γ -³²P]ATP was radiolabeled as described previously (Supplementary Table 1).⁶⁶ In order to generate substrates containing appropriate DSBs, we annealed complementary oligomers (100 mM NaCl and 1 mM EDTA) by incubating them in boiling water for 10 min, followed by slow cooling.⁶⁷ The oligomeric double-stranded DNA containing 5' overhangs (compatible ends) were prepared by annealing a [γ -³²P]ATP end-labeled 75-nt oligomer, TSK1, with an unlabeled complementary oligomer, TSK2. Similarly, 5'-5'-noncompatible and 5'-3'-noncompatible overhangs were prepared by annealing end-labeled TSK1 with unlabeled VK11 and VK13, respectively. Blunt-end substrate was prepared by annealing labeled 75-mer VK7 with unlabeled VK8.³⁹ Substrates containing 13-nt microhomology were prepared by annealing SS69 with SS70 and by annealing SS71 with SS72.

NHEJ assay

NHEJ assay was performed by incubating 4 nM radiolabeled oligomeric DNA with 5 μg of cell-free extracts in a buffer containing 30 mM HEPES-KOH (pH 7.9), 7.5 mM MgCl_2 , 1 mM DTT, 2 mM ATP, 50 μM dNTPs, and 0.1 μg of bovine serum albumin in a reaction volume of 10 μl (Supplementary Fig. 2) at 37°C for 1, 2, or 6 h, as specified.^{39,54} NHEJ reaction was arrested (10 mM EDTA and Proteinase K), and DNA was purified by phenol-chloroform extraction. The reaction products were resolved on 8% denaturing PAGE, which was dried and exposed. The signal was detected using PhosphorImager (FLA9000; Fuji, Japan) and analyzed with Multi Gauge (V3.0) program.

In the case of substrates containing 13-nt microhomology, following NHEJ reaction, the joined products were amplified using radiolabeled primer SS60 and unlabeled primer SS61. Reaction products were resolved on 8% denaturing PAGE, as described above.

PCR amplification, cloning, and sequencing of NHEJ junctions

End-joined products such as dimers, trimers, and multimers were cut out from the gel, eluted, and used for PCR amplification of NHEJ junctions using primers

VK24 and SS37, as described previously.^{39,54} In the case of substrates containing microhomology, following NHEJ reaction, the joined products were amplified using primers SS60 and SS61. PCR products were purified and cloned into the TA vector. The presence of insert was verified by restriction enzyme digestion and subjected to sequencing (Macrogen, Inc., South Korea).

Immunoblot analysis

For immunoblotting analysis, 40–50 µg of protein was resolved on 7–10% SDS-PAGE.⁶⁸ Following electrophoresis, proteins were transferred to a PVDF membrane (Millipore, USA) and probed with appropriate primary antibodies against KU70, KU80, DNA-PKcs, XRCC4, ligase IV, Pol λ, MRE11, RAD50, NBS1, RAD51, p73, p53, BCL2, pATM, ligase III, CtIP, cyclin B1, cyclin D1, and with appropriate secondary antibodies, as per standard protocol. Tubulin was used as internal loading control. The blots were developed using chemiluminescent solution (Immobilon™ western; Millipore) and scanned by a gel documentation system (LAS 3000; Fuji, Japan).

Quantification

For quantification of bands of interest, Multi Gauge (V3.0) software was used as described previously.⁶⁷ A rectangle covering the band of interest was selected, and intensity was quantified. A similar rectangle was then placed over other bands of interest in each lane, quantified, and added. An equal area from the same lane of the blot where no specific band was present was used as background and subtracted. The intensity obtained from each lane was plotted and presented as a bar diagram.

Immunoprecipitation assay

Immunoprecipitation experiments were performed as described earlier.^{39,54} Protein G agarose beads (Sigma) were incubated with the appropriate antibody (0.04 µg/µl) overnight in immunoprecipitation buffer [0.5 M NaCl, 10 mM Tris (pH 7.5), and 0.2% NP40]. The beads were spun down, and the supernatant was removed. Ten micrograms of 14.5-day cephalon was then mixed with antibody-bound beads and incubated overnight. Protein depletion was confirmed in the resulting supernatant by immunoblot analysis and quantified using Multi Gauge (V3.0). This immunodepleted extract was used for NHEJ assays.

Immunofluorescence staining

Embryos aged 9.5, 14.5, and 18.5 days were collected as described above and stored in 4% paraformaldehyde at 4 °C until use. Histological sections were prepared as per standard protocols⁶⁹ using a rotary microtome (Leica Biosystems, Germany). After being dewaxed in xylene and rehydrated in graded alcohols, the sections were boiled in 10 mM citrate buffer and preincubated with blocking buffer (20% horse serum, 1% bovine serum albumin, and 0.1% Tween 20). Tissue sections were then

incubated with the appropriate antibody [anti-CtIP, anti-ligase III, anti-MRE11, anti-ligase IV, or anti-p53BP1 (1:50)], followed by incubation with biotinylated secondary antibody and addition of streptavidin–fluorescein isothiocyanate. The sections were counterstained with 4,6-diamidino-2-phenylindole, rinsed, dehydrated, and mounted with anti-fade mounting medium. Sections were observed under a fluorescence microscope (Zeiss, Germany) at a magnification of 10× and documented.

Acknowledgements

We thank Dr. Mridula Nambiar, Ms. Nishana M., Ms. Mrinal Srivastava, and other members of the S.C.R. laboratory for discussions and help. This work was supported by grant 2008/37/5/BRNS from DAE (India) and by a IISc start-up grant to S.C.R. K.K.C. was supported by a postdoctoral fellowship from DBT (India).

Conflict of Interest. Authors disclose that there is no conflict of interest.

Supplementary Data

Supplementary data to this article can be found online at [doi:10.1016/j.jmb.2012.01.029](https://doi.org/10.1016/j.jmb.2012.01.029)

References

- Dikomey, E., Dahm-Daphi, J., Brammer, I., Martensen, R. & Kaina, B. (1998). Correlation between cellular radiosensitivity and non-repaired double-strand breaks studied in nine mammalian cell lines. *Int. J. Radiat. Biol.* **73**, 269–278.
- Pfeiffer, P., Goedecke, W. & Obe, G. (2000). Mechanisms of DNA double-strand break repair and their potential to induce chromosomal aberrations. *Mutagenesis*, **15**, 289–302.
- Hoeijmakers, J. H. (2001). Genome maintenance mechanisms for preventing cancer. *Nature*, **411**, 366–374.
- Nambiar, M., Kari, V. & Raghavan, S. C. (2008). Chromosomal translocations in cancer. *Biochim. Biophys. Acta*, **1786**, 139–152.
- Lieber, M. R., Yu, K. & Raghavan, S. C. (2006). Roles of nonhomologous DNA end joining, V(D)J recombination, and class switch recombination in chromosomal translocations. *DNA Repair (Amsterdam)*, **5**, 1234–1245.
- Haber, J. E. (2000). Partners and pathways repairing a double-strand break. *Trends Genet.* **16**, 259–264.
- Karran, P. (2000). DNA double strand break repair in mammalian cells. *Curr. Opin. Genet. Dev.* **10**, 144–150.
- Bassing, C. H., Swat, W. & Alt, F. W. (2002). The mechanism and regulation of chromosomal V(D)J recombination. *Cell*, **109**, S45–S55.
- Lieber, M. R., Ma, Y., Pannicke, U. & Schwarz, K. (2004). The mechanism of vertebrate nonhomologous DNA end joining and its role in V(D)J recombination. *DNA Repair (Amsterdam)*, **3**, 817–826.

10. Chiruvella, K. K., Sankaran, S. K., Singh, M., Nambiar, M. & Raghavan, S. C. (2007). Mechanism of DNA double-strand break repair. *ICFAI J. Biotechnol.* **1**, 7–22.
11. Wyman, C. & Kanaar, R. (2006). DNA double-strand break repair: all's well that ends well. *Annu. Rev. Genet.* **40**, 363–383.
12. Hefferin, M. L. & Tomkinson, A. E. (2005). Mechanism of DNA double-strand break repair by non-homologous end joining. *DNA Repair (Amsterdam)*, **4**, 639–648.
13. Lieber, M. R., Lu, H., Gu, J. & Schwarz, K. (2008). Flexibility in the order of action and in the enzymology of the nuclease, polymerases, and ligase of vertebrate non-homologous DNA end joining: relevance to cancer, aging, and the immune system. *Cell Res.* **18**, 125–133.
14. Yano, K., Morotomi-Yano, K., Adachi, N. & Akiyama, H. (2009). Molecular mechanism of protein assembly on DNA double-strand breaks in the non-homologous end-joining pathway. *J. Radiat. Res. (Tokyo)*, **50**, 97–108.
15. Sharma, S. & Raghavan, S. C. (2010). Nonhomologous DNA end joining in cell-free extracts. *J. Nucleic Acids*, doi: 10.4061/2010/389129.
16. Mimori, T. & Hardin, J. A. (1986). Mechanism of interaction between Ku protein and DNA. *J. Biol. Chem.* **261**, 10375–10379.
17. Falzon, M., Fewell, J. W. & Kuff, E. L. (1993). EBP-80, a transcription factor closely resembling the human autoantigen Ku, recognizes single- to double-strand transitions in DNA. *J. Biol. Chem.* **268**, 10546–10552.
18. West, R. B., Yaneva, M. & Lieber, M. R. (1998). Productive and nonproductive complexes of Ku and DNA-dependent protein kinase at DNA termini. *Mol. Cell. Biol.* **18**, 5908–5920.
19. Ma, Y., Pannicke, U., Schwarz, K. & Lieber, M. R. (2002). Hairpin opening and overhang processing by an Artemis/DNA-dependent protein kinase complex in nonhomologous end joining and V(D)J recombination. *Cell*, **108**, 781–794.
20. Ma, Y., Lu, H., Tippin, B., Goodman, M. F., Shimazaki, N., Koiwai, O. *et al.* (2004). A biochemically defined system for mammalian nonhomologous DNA end joining. *Mol. Cell*, **16**, 701–713.
21. Nick McElhinny, S. A. & Ramsden, D. A. (2004). Sibling rivalry: competition between Pol X family members in V(D)J recombination and general double strand break repair. *Immunol. Rev.* **200**, 156–164.
22. Tseng, H. M. & Tomkinson, A. E. (2002). A physical and functional interaction between yeast Pol4 and Dnl4–Lif1 links DNA synthesis and ligation in nonhomologous end joining. *J. Biol. Chem.* **277**, 45630–45637.
23. Mahajan, K. N., Nick McElhinny, S. A., Mitchell, B. S. & Ramsden, D. A. (2002). Association of DNA polymerase mu (pol mu) with Ku and ligase IV: role for pol mu in end-joining double-strand break repair. *Mol. Cell. Biol.* **22**, 5194–5202.
24. Grawunder, U., Wilm, M., Wu, X., Kulesza, P., Wilson, T. E., Mann, M. & Lieber, M. R. (1997). Activity of DNA ligase IV stimulated by complex formation with XRCC4 protein in mammalian cells. *Nature*, **388**, 492–495.
25. Wilson, T. E., Grawunder, U. & Lieber, M. R. (1997). Yeast DNA ligase IV mediates non-homologous DNA end joining. *Nature*, **388**, 495–498.
26. Ahnesorg, P., Smith, P. & Jackson, S. P. (2006). XLF interacts with the XRCC4–DNA ligase IV complex to promote DNA nonhomologous end-joining. *Cell*, **124**, 301–313.
27. Bogue, M. A., Wang, C., Zhu, C. & Roth, D. B. (1997). V(D)J recombination in Ku86-deficient mice: distinct effects on coding, signal, and hybrid joint formation. *Immunity*, **7**, 37–47.
28. Zhu, C., Mills, K. D., Ferguson, D. O., Lee, C., Manis, J., Fleming, J. *et al.* (2002). Unrepaired DNA breaks in p53-deficient cells lead to oncogenic gene amplification subsequent to translocations. *Cell*, **109**, 811–821.
29. Boboila, C., Jankovic, M., Yan, C. T., Wang, J. H., Wesemann, D. R., Zhang, T. *et al.* (2010). Alternative end-joining catalyzes robust IgH locus deletions and translocations in the combined absence of ligase 4 and Ku70. *Proc. Natl Acad. Sci. USA*, **107**, 3034–3039.
30. Della-Maria, J., Zhou, Y., Tsai, M. S., Kuhnlein, J., Carney, J., Paull, T. & Tomkinson, A. (2011). hMre11/hRad50/Nbs1 and DNA ligase III{alpha}/XRCC1 act together in an alternative non-homologous end joining pathway. *J. Biol. Chem.* **286**, 33845–33853.
31. Helmink, B. A., Tubbs, A. T., Dorsett, Y., Bednarski, J. J., Walker, L. M., Feng, Z. *et al.* (2011). H2AX prevents CtIP-mediated DNA end resection and aberrant repair in G1-phase lymphocytes. *Nature*, **469**, 245–249.
32. You, Z., Shi, L. Z., Zhu, Q., Wu, P., Zhang, Y. W., Basilio, A. *et al.* (2009). CtIP links DNA double-strand break sensing to resection. *Mol. Cell*, **36**, 954–969.
33. Bothmer, A., Robbiani, D. F., Feldhahn, N., Gazumyan, A., Nussenzweig, A. & Nussenzweig, M. C. (2010). 53BP1 regulates DNA resection and the choice between classical and alternative end joining during class switch recombination. *J. Exp. Med.* **207**, 855–865.
34. Bothmer, A., Robbiani, D. F., Di Virgilio, M., Bunting, S. F., Klein, I. A., Feldhahn, N. *et al.* (2011). Regulation of DNA end joining, resection, and immunoglobulin class switch recombination by 53BP1. *Mol. Cell*, **42**, 319–329.
35. Mac Auley, A., Werb, Z. & Mirkes, P. E. (1993). Characterization of the unusually rapid cell cycles during rat gastrulation. *Development*, **117**, 873–883.
36. Zheng, P., Schramm, R. D. & Latham, K. E. (2005). Developmental regulation and *in vitro* culture effects on expression of DNA repair and cell cycle checkpoint control genes in rhesus monkey oocytes and embryos. *Biol. Reprod.* **72**, 1359–1369.
37. Wurtele, H., Gusew, N., Lussier, R. & Chartrand, P. (2005). Characterization of *in vivo* recombination activities in the mouse embryo. *Mol. Genet. Genomics*, **273**, 252–263.
38. Orii, K. E., Lee, Y., Kondo, N. & McKinnon, P. J. (2006). Selective utilization of nonhomologous end-joining and homologous recombination DNA repair pathways during nervous system development. *Proc. Natl Acad. Sci. USA*, **103**, 10017–10022.
39. Kumar, T. S., Kari, V., Choudhary, B., Nambiar, M., Akila, T. S. & Raghavan, S. C. (2010). Anti-apoptotic

- protein BCL2 down-regulates DNA end joining in cancer cells. *J. Biol. Chem.* **285**, 32657–32670.
40. Yu, X. & Chen, J. (2004). DNA damage-induced cell cycle checkpoint control requires CtIP, a phosphorylation-dependent binding partner of BRCA1 C-terminal domains. *Mol. Cell. Biol.* **24**, 9478–9486.
 41. Huertas, P. & Jackson, S. P. (2009). Human CtIP mediates cell cycle control of DNA end resection and double strand break repair. *J. Biol. Chem.* **284**, 9558–9565.
 42. Baumann, P. & West, S. C. (1998). DNA end-joining catalyzed by human cell-free extracts. *Proc. Natl Acad. Sci. USA*, **95**, 14066–14070.
 43. Hanakahi, L. A., Bartlett-Jones, M., Chappell, C., Pappin, D. & West, S. C. (2000). Binding of inositol phosphate to DNA-PK and stimulation of double-strand break repair. *Cell*, **102**, 721–729.
 44. Sathees, C. R. & Raman, M. J. (1999). Mouse testicular extracts process DNA double-strand breaks efficiently by DNA end-to-end joining. *Mutat. Res.* **433**, 1–13.
 45. Thode, S., Schafer, A., Pfeiffer, P. & Vielmetter, W. (1990). A novel pathway of DNA end-to-end joining. *Cell*, **60**, 921–928.
 46. Budman, J. & Chu, G. (2005). Processing of DNA for nonhomologous end-joining by cell-free extract. *EMBO J.* **24**, 849–860.
 47. Pfeiffer, P. & Vielmetter, W. (1988). Joining of nonhomologous DNA double strand breaks *in vitro*. *Nucleic Acids Res.* **16**, 907–924.
 48. Raghavan, S. C. & Raman, M. J. (2004). Nonhomologous end joining of complementary and noncomplementary DNA termini in mouse testicular extracts. *DNA Repair (Amsterdam)*, **3**, 1297–1310.
 49. Pastwa, E., Somiari, R. I., Malinowski, M., Somiari, S. B. & Winters, T. A. (2009). *In vitro* non-homologous DNA end joining assays—the 20th anniversary. *Int. J. Biochem. Cell Biol.* **41**, 1254–1260.
 50. North, P., Ganesh, A. & Thacker, J. (1990). The rejoining of double-strand breaks in DNA by human cell extracts. *Nucleic Acids Res.* **18**, 6205–6210.
 51. Thacker, J., Chalk, J., Ganesh, A. & North, P. (1992). A mechanism for deletion formation in DNA by human cell extracts: the involvement of short sequence repeats. *Nucleic Acids Res.* **20**, 6183–6188.
 52. Lehman, C. W., Clemens, M., Worthylake, D. K., Trautman, J. K. & Carroll, D. (1993). Homologous and illegitimate recombination in developing *Xenopus* oocytes and eggs. *Mol. Cell. Biol.* **13**, 6897–6906.
 53. Labhart, P. (1999). Nonhomologous DNA end joining in cell-free systems. *Eur. J. Biochem.* **265**, 849–861.
 54. Sharma, S., Choudhary, B. & Raghavan, S. C. (2011). Efficiency of nonhomologous DNA end joining varies among somatic tissues, despite similarity in mechanism. *Cell. Mol. Life Sci.* **68**, 661–676.
 55. Derbyshire, M. K., Epstein, L. H., Young, C. S., Munz, P. L. & Fishel, R. (1994). Nonhomologous recombination in human cells. *Mol. Cell. Biol.* **14**, 156–169.
 56. Lieber, M. R. & Karanjawala, Z. E. (2004). Ageing, repetitive genomes and DNA damage. *Nat. Rev. Mol. Cell Biol.* **5**, 69–75.
 57. Lee, J. W., Blanco, L., Zhou, T., Garcia-Diaz, M., Bebenek, K., Kunkel, T. A. *et al.* (2004). Implication of DNA polymerase lambda in alignment-based gap filling for nonhomologous DNA end joining in human nuclear extracts. *J. Biol. Chem.* **279**, 805–811.
 58. Fairman, M. P., Johnson, A. P. & Thacker, J. (1992). Multiple components are involved in the efficient joining of double stranded DNA breaks in human cell extracts. *Nucleic Acids Res.* **20**, 4145–4152.
 59. Nicolas, A. L., Munz, P. L. & Young, C. S. (1995). A modified single-strand annealing model best explains the joining of DNA double-strand breaks mammalian cells and cell extracts. *Nucleic Acids Res.* **23**, 1036–1043.
 60. Daza, P., Reichenberger, S., Gottlich, B., Hagmann, M., Feldmann, E. & Pfeiffer, P. (1996). Mechanisms of nonhomologous DNA end-joining in frogs, mice and men. *Biol. Chem.* **377**, 775–786.
 61. Cang, Y., Zhang, J., Nicholas, S. A., Kim, A. L., Zhou, P. & Goff, S. P. (2007). DDB1 is essential for genomic stability in developing epidermis. *Proc. Natl Acad. Sci. USA*, **104**, 2733–2737.
 62. Lieber, M. R. (2010). The mechanism of double-strand DNA break repair by the nonhomologous DNA end-joining pathway. *Annu. Rev. Biochem.* **79**, 181–211.
 63. Quennet, V., Beucher, A., Barton, O., Takeda, S. & Lobrich, M. (2010). CtIP and MRN promote non-homologous end-joining of etoposide-induced DNA double-strand breaks in G1. *Nucleic Acids Res.* **39**, 2144–2152.
 64. Sallmyr, A., Tomkinson, A. E. & Rassool, F. V. (2008). Up-regulation of WRN and DNA ligase IIIalpha in chronic myeloid leukemia: consequences for the repair of DNA double-strand breaks. *Blood*, **112**, 1413–1423.
 65. Liang, L., Deng, L., Nguyen, S. C., Zhao, X., Maulion, C. D., Shao, C. & Tischfield, J. A. (2008). Human DNA ligases I and III, but not ligase IV, are required for microhomology-mediated end joining of DNA double-strand breaks. *Nucleic Acids Res.* **36**, 3297–3310.
 66. Naik, A. K. & Raghavan, S. C. (2008). P1 nuclease cleavage is dependent on length of the mismatches in DNA. *DNA Repair (Amsterdam)*, **7**, 1384–1391.
 67. Naik, A. K., Lieber, M. R. & Raghavan, S. C. (2010). Cytosines, but not purines, determine recombination activating gene (RAG)-induced Breaks on heteroduplex DNA structures: implications for genomic instability. *J. Biol. Chem.* **285**, 7587–7597.
 68. Chiruvella, K. K., Kari, V., Choudhary, B., Nambiar, M., Ghanta, R. G. & Raghavan, S. C. (2008). Methyl angolensate, a natural tetranortriterpenoid induces intrinsic apoptotic pathway in leukemic cells. *FEBS Lett.* **582**, 4066–4076.
 69. Wheeler, P. R., Burkitt, H. G. & Daniels, V. G. (1987). *Functional Histology: A Text and Colour Atlas*, 2nd edit. Churchill Livingstone, London, UK.